S XI EMISSION LINES IN ACTIVE REGION SPECTRA OBTAINED WITH THE SOLAR EUV ROCKET TELESCOPE AND SPECTROGRAPH (SERTS)

F. P. KEENAN[1], D. J. PINFIELD[1], M. MATHIOUDAKIS[1], K. M. AGGARWAL[1], R. J. THOMAS[2] and J. W. BROSIUS[2,3]

[1]*Department of Pure and Applied Physics, The Queen's University of Belfast, Belfast BT7 1NN, Northern Ireland*

[2]*Laboratory for Astronomy and Solar Physics, Code 682, NASA's/Goddard Space Flight Center, Greenbelt, MD 20771, U.S.A.*

[3]*Raytheon ITSS, Lanham, MD 20706, U.S.A.*

(Received 11 July 2000; accepted 6 September 2000)

Abstract. Theoretical electron density sensitive emission line ratios involving a total of eleven $2s^2 2p^2 - 2s2p^3$ transitions in S XI between 187 and 292 Å are presented. A comparison of these with solar active region observations obtained during rocket flights by the Solar EUV Rocket Telescope and Spectrograph (SERTS) reveals generally good agreement between theory and experiment. However, the 186.87 Å line is masked by fairly strong Fe XII emission at the same wavelength, while 239.83 Å is blended with an unknown feature, and 285.58 Å is blended with possibly N IV 285.56 Å. In addition, the 191.23 Å line appears to be more seriously blended with an Fe XIII feature than previously believed. The presence of several new S XI lines is confirmed in the SERTS spectra, at wavelengths of 188.66, 247.14 and 291.59 Å, in excellent agreement with laboratory measurements. In particular, the detection of the $2s^2 2p^2\ ^3P_1 - 2s2p^3\ ^3P_{0,1}$ transitions at 242.91 Å is the first time (to our knowledge) that this feature has been identified in the solar spectrum. The potential usefulness of the S XI line ratios as electron density diagnostics for the solar transition region and corona is briefly discussed.

1. Introduction

Emission lines arising from $2s^2 2p^2 - 2s2p^3$ transitions in carbon-like ions are frequently detected in solar ultraviolet spectra (Dere, 1982; Vernazza and Reeves, 1978). They may be used to determine the electron temperature and/or density of the solar transition region and corona through diagnostic line ratios, as pointed out by Mason and Bhatia (1978) and Mason *et al.* (1979). However, to calculate reliable theoretical ratios, accurate atomic data must be employed, for electron and proton impact excitation rates and Einstein A-coefficients (Mason and Monsignori-Fossi, 1994).

In this paper we present new calculations of electron density sensitive line ratios for S XI. We compare these with active region observations obtained with the Solar EUV Rocket Telescope and Spectrograph (SERTS), in order to identify weak S XI

Solar Physics **197:** 253–262, 2000.

emission features in the solar spectrum, and investigate the importance of blending for these lines.

2. Theoretical Line Ratios

The model ion for S XI consisted of the nine energetically lowest LS states, namely $2s^2 2p^2\ ^3P$, ^1D and ^1S, $2s2p^3\ ^5S$, ^3D, ^3P, ^1D, ^3S and ^1P, making a total of 15 levels when the fine-structure splitting is included. Energies of all these levels were obtained from Kaufman and Martin (1993). Test calculations including the higher lying $2p^4$ states were found to have a negligible effect on theoretical line ratios involving transitions between $2s^2 2p^2$ and $2s2p^3$.

Electron impact excitation rates for transitions in S XI were taken from Conlon, Keenan, and Aggarwal (1992), while for Einstein A-coefficients the calculations of Aggarwal (1998) and Froese Fischer and Saha (1985) were adopted for allowed lines, and intercombination and forbidden transitions, respectively. As noted by, for example, Seaton (1964), excitation by proton impact is only important for transitions among the $2s^2 2p^2\ ^3P$ levels. In the present analysis, we have employed the proton excitation rates of Ryans *et al.* (1999).

Using the atomic data discussed above in conjunction with the statistical equilibrium code of Dufton (1977), relative S XI level populations and hence emission line strengths were calculated as a function of electron temperature (T_e) and density (N_e). The following assumptions were made in the calculations: (i) that ionization to and recombination from other ionic levels is slow compared with bound-bound rates, (ii) that photoexcitation and de-excitation rates are negligible in comparison with the corresponding collisional rates, (iii) that all transitions are optically thin. Further details of the procedures involved may be found in Dufton (1977) and Dufton *et al.* (1978).

In Figures 1 and 2 we plot the theoretical emission line ratios

$$R_1 = I(2s^2 2p^2\ ^3P_0 - 2s2p^3\ ^3S_1)/I(2s^2 2p^2\ ^3P_1 - 2s2p^3\ ^3D_2)$$

$$= I(186.87\ \text{Å})/I(285.83\ \text{Å}),$$

$$R_2 = I(2s^2 2p^2\ ^3P_2 - 2s2p^3\ ^3P_1)/I(2s^2 2p^2\ ^3P_1 - 2s2p^3\ ^3D_2)$$

$$= I(247.14\ \text{Å})/I(285.83\ \text{Å}),$$

$$R_3 = I(2s^2 2p^2\ ^3P_1 - 2s2p^3\ ^3P_{0,1})/I(2s^2 2p^2\ ^3P_1 - 2s2p^3\ ^3D_2)$$

$$= I(242.91\ \text{Å})/I(285.83\ \text{Å}),$$

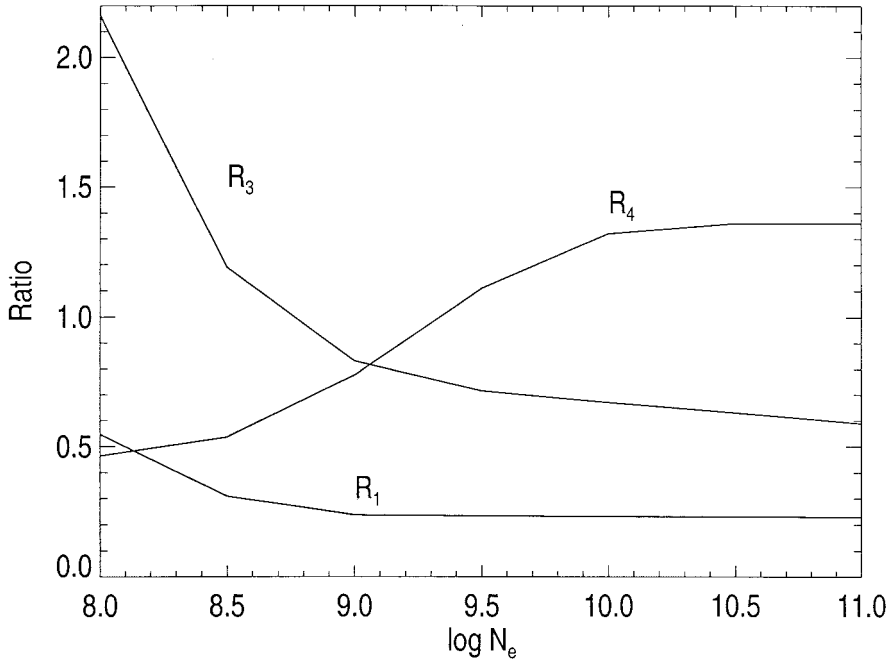

Figure 1. The theoretical S XI emission line ratios
$R_1 = I(2s^2 2p^2\ ^3P_0 - 2s2p^3\ ^3S_1)/I(2s^2 2p^2\ ^3P_1 - 2s2p^3\ ^3D_2) = I(186.87\ \text{Å})/I(285.83\ \text{Å})$,
$R_3 = I(2s^2 2p^2\ ^3P_1 - 2s2p^3\ ^3P_{0,1})/I(2s^2 2p^2\ ^3P_1 - 2s2p^3\ ^3D_2) = I(242.91\ \text{Å})/I(285.83\ \text{Å})$, and
$R_4 = I(2s^2 2p^2\ ^3P_2 - 2s2p^3\ ^3D_3)/I(2s^2 2p^2\ ^3P_1 - 2s2p^3\ ^3D_2) = I(291.59\ \text{Å})/I(285.83\ \text{Å})$, where I is in energy units, plotted as a function of logarithmic electron density (N_e in cm^{-3}) at the temperature of maximum S XI fractional abundance in ionization equilibrium, $T_e = 1.8 \times 10^6$ K (Mazzotta *et al.*, 1998).

$$R_4 = I(2s^2 2p^2\ ^3P_2 - 2s2p^3\ ^3D_3)/I(2s^2 2p^2\ ^3P_1 - 2s2p^3\ ^3D_2)$$
$$= I(291.59\ \text{Å})/I(285.83\ \text{Å}),$$
$$R_5 = I(2s^2 2p^2\ ^3P_2 - 2s2p^3\ ^3P_2)/I(2s^2 2p^2\ ^3P_1 - 2s2p^3\ ^3D_2)$$
$$= I(246.89\ \text{Å})/I(285.83\ \text{Å}),$$

and

$$R_6 = I(2s^2 2p^2\ ^3P_0 - 2s2p^3\ ^3D_1)/I(2s^2 2p^2\ ^3P_1 - 2s2p^3\ ^3D_2)$$
$$= I(281.44\ \text{Å})/I(285.83\ \text{Å})$$

as a function of electron density at the temperature of maximum S XI fractional abundance in ionization equilibrium, $T_e = 1.8 \times 10^6$ K (Mazzotta *et al.*, 1998). Given errors in the adopted atomic data of typically $\pm 10\%$ (see above references),

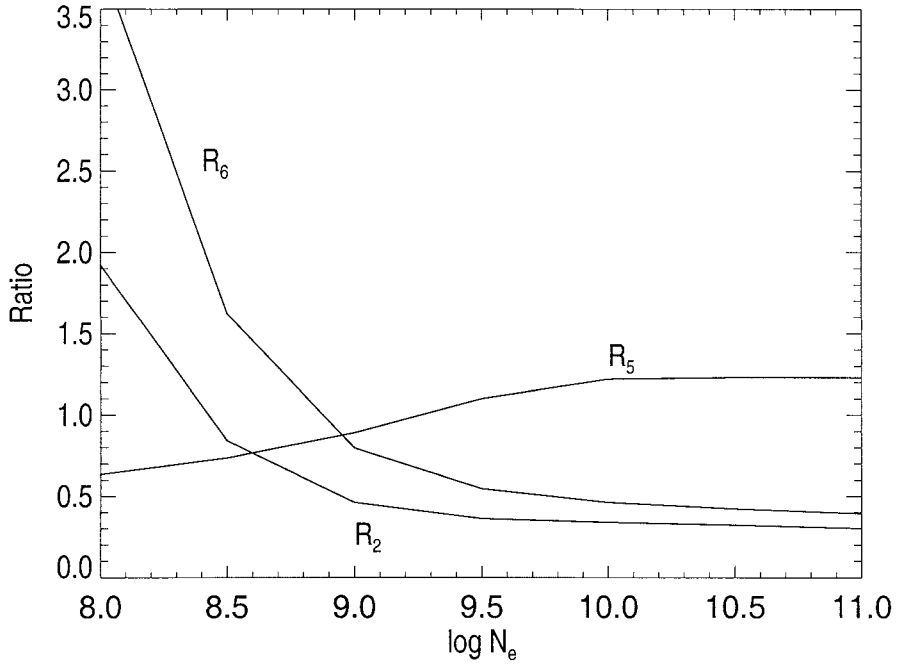

Figure 2. The theoretical S XI emission line ratios
$R_2 = I(2s^2 2p^2\ ^3P_2 - 2s2p^3\ ^3P_1)/I(2s^2 2p^2\ ^3P_1 - 2s2p^3\ ^3D_2) = I(247.14\ \text{Å})/I(285.83\ \text{Å})$,
$R_5 = I(2s^2 2p^2\ ^3P_2 - 2s2p^3\ ^3P_2)/I(2s^2 2p^2\ ^3P_1 - 2s2p^3\ ^3D_2) = I(246.89\ \text{Å})/I(285.83\ \text{Å})$, and
$R_6 = I(2s^2 2p^2\ ^3P_0 - 2s2p^3\ ^3D_1)/I(2s^2 2p^2\ ^3P_1 - 2s2p^3\ ^3D_2) = I(281.44\ \text{Å})/I(285.83\ \text{Å})$, where I is in energy units, plotted as a function of logarithmic electron density (N_e in cm^{-3}) at the temperature of maximum S XI fractional abundance in ionization equilibrium, $T_e = 1.8 \times 10^6$ K (Mazzotta *et al.*, 1998).

we would expect the theoretical ratios to be accurate to better than $\pm 20\%$. An inspection of the figures reveals that the ratios are sensitive to variations in the electron density, with for example R_2 and R_6 varying by factors of 6.4 and 9.7, respectively, between $N_e = 10^8$ and 10^{11} cm^{-3}. However, the ratios are relatively insensitive to changes in the adopted electron temperature. For example, reducing T_e from 1.8×10^6 K to 10^6 K leads to only a 20% and 15% variation in R_2 and R_6, respectively, at $N_e = 10^8$ cm^{-3}, decreasing to 11% and 4% at $N_e = 10^{11}$ cm^{-3}. This sensitivity to changes in the electron density, but not temperature, indicates that the ratios should, in principle, be useful N_e–diagnostics for the S XI emitting region of a plasma.

We note that the ratios

$$R_7 = I(2s^2 2p^2\ ^3P_1 - 2s2p^3\ ^3S_1)/I(2s^2 2p^2\ ^3P_1 - 2s2p^3\ ^3D_2)$$

$$= I(188.66\ \text{Å})/I(285.83\ \text{Å}),$$

$$R_8 = I(2s^2 2p^2\ ^3P_2 - 2s2p^3\ ^3S_1)/I(2s^2 2p^2\ ^3P_1 - 2s2p^3\ ^3D_2)$$

$$= I(191.23\ \text{Å})/I(285.83\ \text{Å}),$$

$$R_9 = I(2s^2 2p^2\ ^3P_0 - 2s2p^3\ ^3P_1)/I(2s^2 2p^2\ ^3P_1 - 2s2p^3\ ^3D_2)$$

$$= I(239.83\ \text{Å})/I(285.83\ \text{Å}),$$

and

$$R_{10} = I(2s^2 2p^2\ ^3P_1 - 2s2p^3\ ^3D_1)/I(2s^2 2p^2\ ^3P_1 - 2s2p^3\ ^3D_2)$$

$$= I(285.58\ \text{Å})/I(285.83\ \text{Å})$$

have the same temperature and density dependence as R_1, R_2 and R_6 owing to common upper levels, but with

$$R_7 = 2.96 \times R_1, \quad R_8 = 5.13 \times R_1, \quad R_9 = 0.901 \times R_2, \text{ and } R_{10} = 0.495 \times R_6.$$

3. Observational Data

The solar spectra analysed in the present paper are those of active regions NOAA 5464 and 7870, obtained with SERTS, which is discussed in detail by Neupert *et al.* (1992). These spectra were recorded on Eastman Kodak 101-07 emulsion by SERTS during rocket flights on 5 May 1989 at 17:50 UT (SERTS-89) and 15 May 1995 at 18:05 UT (SERTS-95). The SERTS-89 observations cover the wavelength region 235–449 Å in first order and 170–224 Å in second order (the short wavelength cutoff in the latter being due to an absorption edge in the thin aluminium filter installed to reduce stray light), with a spatial resolution of about 7 arc sec (FWHM) and a spectral resolution of 50–80 mÅ (FWHM) in first order and $\leq$ 40 mÅ in second. SERTS-95, which incorporated a multilayer-coated diffraction grating that enhanced the instrumental sensitivity in the second order waveband, observed the 235–335 Å wavelength range in first order and 171–225 Å in second order, at spectral resolutions of 55 mÅ and 30 mÅ, respectively. The SERTS-89 and SERTS-95 active region measurements have been spatially averaged over the central 4.60 and 3.76 arc min of the spectrograph slit, respectively, and wavelength calibrated and converted to absolute intensities using procedures described by Thomas and Neupert (1994) and Brosius, Davila, and Thomas (1998a, b).

TABLE I

S XI transitions and emission line ratios in the SERTS-89 spectrum

Transition	λ (Å)	$R = I(\lambda)/I(285.83$ Å)		Ratio designation
		Observed [a]	Theoretical [b]	
$2s^2 2p^2\ ^3P_2 - 2s2p^3\ ^3S_1$	191.23	4.2 ± 2.2	1.2 ± 0.2	R_8
$2s^2 2p^2\ ^3P_0 - 2s2p^3\ ^3P_1$	239.83	1.9 ± 0.9	0.32 ± 0.06	R_9
$2s^2 2p^2\ ^3P_2 - 2s2p^3\ ^3P_2$	246.89	1.5 ± 0.7	1.2 ± 0.2	R_5
$2s^2 2p^2\ ^3P_0 - 2s2p^3\ ^3D_1$	281.44	0.53 ± 0.27	0.49 ± 0.10	R_6
$2s^2 2p^2\ ^3P_1 - 2s2p^3\ ^3D_1$	285.58	0.78 ± 0.32	0.24 ± 0.05	R_{10}
$2s^2 2p^2\ ^3P_1 - 2s2p^3\ ^3D_2$	285.83	–	–	–

[a] $I(285.83$ Å$) = 84.8 \pm 20.5$ erg cm^{-2} s^{-1} sr^{-1}.
[b] Determined from Figures 1 and 2 at log $N_e = 9.7$.

TABLE II

S XI transitions and emission line ratios in the SERTS-95 spectrum

Transition	λ (Å)	$R = I(\lambda)/I(285.83$ Å)		Ratio designation
		Observed [a]	Theoretical [b]	
$2s^2 2p^2\ ^3P_0 - 2s2p^3\ ^3S_1$	186.87	4.1 ± 1.0	0.24 ± 0.05	R_1
$2s^2 2p^2\ ^3P_1 - 2s2p^3\ ^3S_1$	188.66	0.68 ± 0.17	0.71 ± 0.14	R_7
$2s^2 2p^2\ ^3P_1 - 2s2p^3\ ^3P_{0,1}$	242.91	0.79 ± 0.22	0.73 ± 0.15	R_3
$2s^2 2p^2\ ^3P_2 - 2s2p^3\ ^3P_1$	247.14	0.78 ± 0.30	0.40 ± 0.08	R_2
$2s^2 2p^2\ ^3P_1 - 2s2p^3\ ^3D_2$	285.83	–	–	–
$2s^2 2p^2\ ^3P_2 - 2s2p^3\ ^3D_3$	291.59	0.73 ± 0.29	1.0 ± 0.2	R_4

[a] $I(285.83$ Å$) = 127 \pm 29.8$ erg cm^{-2} s^{-1} sr^{-1}.
[b] Determined from Figures 1 and 2 at log $N_e = 9.4$.

Transitions in S XI identified in the SERTS-89 and SERTS-95 spectra are listed in Tables I and II, respectively. Intensities of these features were determined by using the spectrum synthesis package DIPSO (Howarth, Murray, and Mills, 1994) to fit gaussian profiles to the observations. The intensities of the 285.83 Å line are listed in Tables I and II; the observed intensities of the other S XI transitions may be inferred from these using the line ratios given in the tables (see Section 2). Observational uncertainties in the line ratios have been determined using methods discussed in detail by Thomas and Neupert (1994). A recent re-evaluation of the absolute calibration scale for SERTS-89 increases all active region intensities by a factor of 1.24 over the values reported by Thomas and Neupert, and has been incorporated in the present work.

The quality of the observational data are illustrated in Figures 3 and 4, where we plot the SERTS-95 spectrum between 242.6–243.2 Å and the SERTS-89 data from 285.4–286.0 Å, respectively.

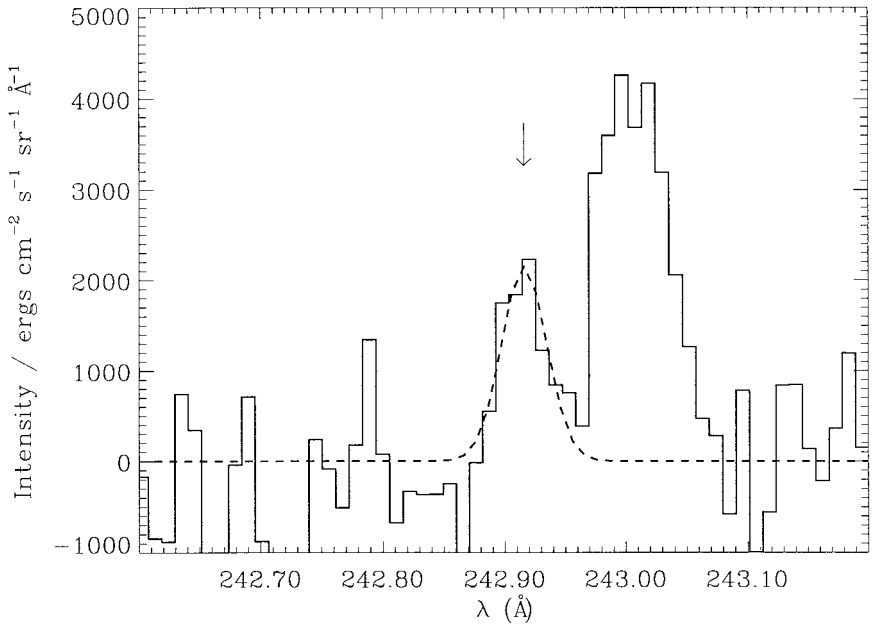

Figure 3. Plot of the SERTS-95 active region spectrum in the 242.6−243.2 Å wavelength range, where the S XI 242.91 Å emission line is indicated by an arrow. The profile fit to the S XI feature is shown by a dashed line. Also clearly visible in the figure is the He II 243.02 Å emission line.

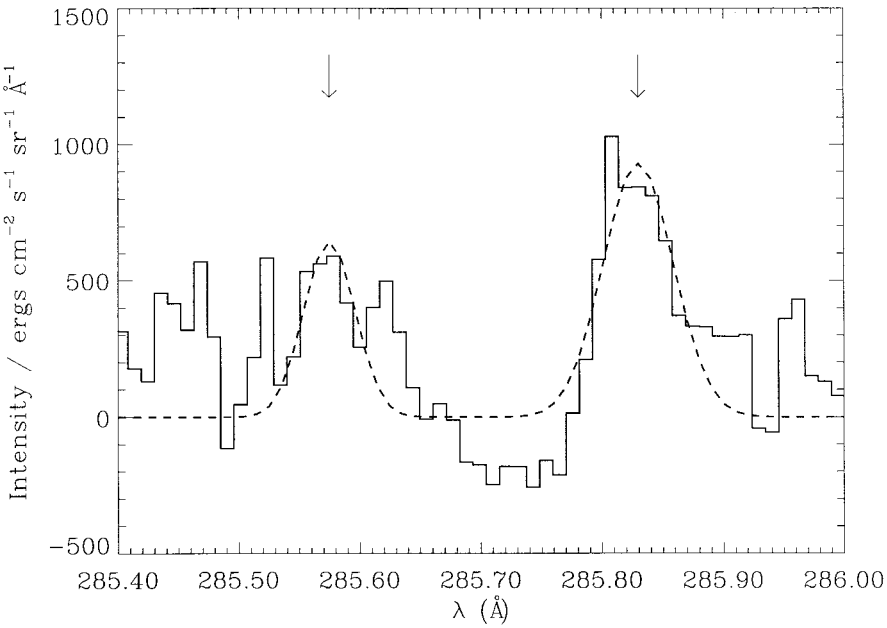

Figure 4. Plot of the SERTS-89 active region spectrum in the 285.4−286.0 Å wavelength range, where the S XI 285.58 and 285.83 Å emission lines are indicated by arrows. The profile fits to the S XI features are shown by a dashed line.

4. Results and Discussion

In Tables I and II we list the observed S XI emission line ratios measured from the SERTS-89 and SERTS-95 spectra, along with the associated 1σ errors. Also shown in Tables I and II are the theoretical results from Figures 1 and 2 for log $N_e = 9.7$ and 9.4, respectively, which we have assumed have an uncertainty of $\pm 20\%$ (see Section 2). These densities have been derived for the SERTS-89 and SERTS-95 active regions from emission lines of Fe XII (Keenan *et al.*, 1996) and Fe XIII (Brosius, Davila, and Thomas, 1998b), respectively, which have temperatures of maximum fractional abundance in ionization equilibrium of T_e(Fe XII) = 1.5×10^6 K and T_e(Fe XIII) = 1.6×10^6 K (Mazzotta *et al.*, 1998), very close to that for S XI. Hence, the Fe XII and Fe XIII densities should reflect that of the S XI emitting plasma in the active regions.

An inspection of Tables I and II reveals large discrepancies between theory and observation for R_1, R_8, R_9 and R_{10}. The 186.87 Å line in R_1 is masked by an Fe XII transition at the same wavelength, which contributes most of the line flux (Young, Landi, and Thomas, 1998). In fact, Brosius, Davila, and Thomas (1998b) list this feature as being due entirely to Fe XII, an interpretation that is consistent within their measurement uncertainties.

Young, Landi, and Thomas (1998) suggest that the 191.23 Å line of S XI is only weakly blended with an Fe XIII transition. However, the large discrepancy between our observed and theoretical values of R_8 would appear to indicate that the 191.23 Å line is more severely blended than previously believed.

Our results also imply that the S XI 239.83 Å line in ratio R_9 is seriously affected by blending, which had not previously been reported. A search of line lists reveals an Fe VII line at 239.85 Å (Kelly, 1987), but no other Fe VII features are reliably detected in any SERTS spectrum. Therefore, the source of blending at 239.83 Å must be considered as unknown at present.

The discrepancy in ratio R_{10} indicates that the S XI 285.58 Å line may be blended as well. This possibility had already been noted by Young, Landi, and Young (1998), but they were not able to offer any plausible source candidates. We suggest that the blend could be with a N IV transition given by Kelly (1987) at a wavelength of 285.56 Å. Although Thomas and Neupert (1994) did not list any lines of N IV in their original analysis of the SERTS-89 spectrum, Keenan *et al.* (1996) found the possible presence of N IV 283.49 Å, with an intensity of 79.6 ± 21.0 erg cm^{-2} s^{-1} sr^{-1}. The intensity ratio of this line to the 285.58 Å feature, I(283.49 Å)/I(285.58 Å) = 1.2 ± 0.5, is quite close to the theoretical N IV ratio of 0.5 (Feldman *et al.*, 1992), indicating that these N IV lines may be present in the SERTS-89 spectrum. Clearly, higher resolution and/or signal-to-noise observations of the solar spectrum in the region of the 239.83 and 285.58 Å lines are desirable, to investigate the possible blending of these features.

For the remainder of the S XI transitions in Tables I and II, the good agreement between the observed and theoretical line ratios imply that these features have

been reliably identified in the SERTS spectra. In particular, we note that we have confirmed the identifications of the 188.66 and 247.14 Å lines by Brosius, Davila, and Thomas (1998b). Malinovsky and Heroux (1973) determined a wavelength of 247.18 Å for the latter, but we note that our value is in much better agreement with the laboratory measurement of 247.12 Å (Podobedova, Kononov, and Koshelev, 1971). We also point out that Behring *et al.* (1976) identified a line at 247.17 Å in their solar spectrum as being due to N IV. However, the intensity ratio of this feature to that of the S XI 285.83 Å transition (0.38) is in excellent agreement with the theoretical value of R_2 in Table II, indicating that the 247.17 Å line in Behring *et al.* is in fact due to S XI. An additional confirmation comes from the re-analysis of the SERTS-89 spectrum by Young, Landi, and Thomas (1998), who found a feature at 247.16 Å that is within 1σ of the expected intensity for S XI.

Our measurement of the S XI line at 291.59 Å confirms the tentative identification of this feature in the solar spectrum by Malinovsky and Heroux (1973) at 291.63 Å. However, the SERTS-95 wavelength is in much better agreement with the laboratory determination of 291.59 Å by Podobedova, Kononov, and Koshelev (1971). Our detection of the 242.91 Å line is (to our knowledge) the first time that this feature has been identified in the Sun, although both Behring, Cohen, and Feldman (1972) and Behring *et al.* (1976) list an unidentified line at 242.85 Å. The measured solar wavelength for this feature is in moderate agreement with the laboratory value of 242.82 Å (Podobedova, Kononov, and Koshelev, 1971), and with the predicted wavelength pair of 242.85 and 242.87 Å from CHIANTI (Young, Landi, and Thomas, 1998).

Finally, we noted in Section 2 that the R_1 through R_{10} ratios are sensitive to variations in electron density, but not temperature, and hence in principle should make useful N_e-diagnostics. However, the line intensities would need to be measured to a much higher accuracy than possible from the SERTS-89 or SERTS-95 spectra, for reliable density estimates to be obtained. The typical uncertainty in the SERTS line ratios is $\pm$ 40%, corresponding to over an order of magnitude variation in N_e for the ratios in Figures 1 and 2. However, measurements of R_1 through R_{10} to an accuracy of $\pm$10% could lead to density estimates reliable to $\pm$ 0.2 dex.

Acknowledgements

DJP acknowledges financial support from the Leverhulme Trust. The SERTS rocket programme is funded under NASA RTOP 344-17-38.

References

Aggarwal, K. M.: 1998, *Astrophys. J. Suppl.* **118**, 589.
Brosius, J. W., Davila, J. M., and Thomas, R. J.: 1998a, *Astrophys. J.* **497**, L113.
Brosius, J. W., Davila, J. M., and Thomas, R. J.: 1998b, *Astrophys. J. Suppl.* **119**, 255.

Behring, W. E., Cohen, L., and Feldman, U.: 1972, *Astrophys. J.* **175**, 493.
Behring, W. E., Cohen, L., Feldman, U., and Doschek, G. A.: 1976, *Astrophys. J.* **203**, 521.
Conlon, E. S., Keenan, F. P., and Aggarwal, K. M.: 1992, *Phys. Scripta* **45**, 309.
Dere, K. P.: 1982, *Solar Phys.* **77**, 77.
Dufton, P. L.: 1977, *Comp. Phys. Comm.* **13**, 25.
Dufton, P. L., Berrington, K. A., Burke, P. G., and Kingston, A. E.: 1978, *Astron. Astrophys.* **62**, 111.
Feldman, U., Mandelbaum, P., Seely, J. F., Doschek, G. A., and Gursky, H.: 1992, *Astrophys. J. Suppl.* **81**, 387.
Froese Fischer, C. and Saha, H. P.: 1985, *Phys. Scripta* **32**, 181.
Howarth, I. D., Murray, J., and Mills, D.: 1994, *Starlink User Note No. 50.15*.
Kaufman, V. and Martin, W. C.: 1993, *J. Phys. Chem. Ref. Data* **22**, 279.
Keenan, F. P., Thomas, R. J., Neupert, W. M., Foster, V. J., Brown, P. J. F., and Tayal, S. S.: 1996, *Monthly Notices Royal Astron. Soc.* **278**, 773.
Kelly, R. L.: 1987, *J. Phys. Chem. Ref. Data*, Suppl. 1.
Malinovsky, M. and Heroux, L.: 1973, *Astrophys. J.* **181**, 1009.
Mason, H. E. and Bhatia, A. K.: 1978, *Monthly Notices Royal Astron. Soc.* **184**, 423.
Mason, H. E., Doschek, G.A., Feldman, U., and Bhatia, A. K.: 1979, *Astron. Astrophys.* **73**, 74.
Mason, H. E. and Monsignori-Fossi, B. C.: 1994, *Astron. Astrophys. Rev.* **6**, 123.
Mazzotta, P., Mazzitelli, G., Colafrancesco, S., and Vittorio, N.: 1998, *Astron. Astrophys. Suppl.* **133**, 403.
Neupert, W. M., Epstein, G. L., Thomas, R. J., and Thompson, W. T.: 1992, *Solar Phys.* **137**, 87.
Podobedova, L. I., Kononov, E. Y., and Koshelev, K. N.: 1971, *Optics Spectr.* **30**, 217.
Ryans, R. S. I., Foster-Woods, V. J., Keenan, F. P., and Reid, R. H. G.: 1999, *Atomic Data Nucl. Data Tables* **73**, 1.
Seaton, M. J.: 1964, *Monthly Notices Royal Astron. Soc.* **127**, 191.
Thomas, R. J. and Neupert, W. M.: 1994, *Astrophys. J. Suppl.* **91**, 461.
Vernazza, J. E. and Reeves, E. M.: 1978, *Astrophys. J. Suppl.* **37**, 485.
Young, P. R., Landi, E., and Thomas, R. J.: 1998, *Astron. Astrophys.* **329**, 291.